Relations between Asphaltene Structures and Their Physical and Chemical Properties: The Rosary-Type Structure

Sócrates Acevedo,* Alexandra Castro, Juan Gabriel Negrin, Alberto Fernández, Gastón Escobar, and Vincent Piscitelli

Universidad Central de Venezuela, Facultad de Ciencias, Escuela de Química, 40756 Caracas 1053, Venezuela

Frederic Delolme and Guy Dessalces

Service Central d'Analyses du CNRS, BP 22 69390 Vernaison, France

Received February 16, 2007. Revised Manuscript Received April 16, 2007

The proposition of the hypothesis-relating structure with properties of asphaltenes is a very important endeavor. In view of their complexity, being an intricate mixture of high-molecular-mass compounds, experimental and theoretical procedures must be designed to check whether the structures proposed are consistent with expected and found behavior. During recent years, a structural characteristic of asphaltene, whereby the several polycyclic systems present in them are joined by flexible aliphatic chains, has been proposed by several authors. For simplicity, we will refer to this as the rosary-type structure. In this paper, using both reported as well as new experimental and theoretical results, an attempt is made to show how asphaltene properties, such as molecular-mass distribution, molecular fragmentation, solubility, adsorption, trapping of molecules, solvent swelling, and aging, could be accounted for in terms of the above rosary-type structures.

Introduction

The asphaltene structure has been the subject of many studies in the past.[1−9] The main target of these studies has been the proposition of structural factors consistent with the limited experimental information available. The usual strategy is to isolate asphaltenes from the crude oil and measure some properties such as the elemental composition, the molecular mass, and spectroscopy properties, such as nuclear magnetic resonance (NMR) for both ^{1}H and ^{13}C. After these properties have been determined, hypothetical structures, consistent with the experimental information are then proposed. Chemical methods have also been employed, in particular by Strausz and co-workers.[1,3,5] Figure 1 is a collection of several of these structures reported in the literature. Beyond the merits, limitations, and meaning of these structures, the important point is whether these are consistent with the expected and measured physical and chemical properties of asphaltenes.

In this regard, it has been suggested that the large difference in solubility in toluene at room temperature between asphaltene fraction A1 (0.09 g L^{-1}) and fraction A2 (between 50 and 100 g L^{-1} depending upon the sample) is not due to differences in molecular mass, aromaticity, or heteroatom content. Differences in these parameters were too small to account for the large difference in solubility.[10−11] Rather, this difference could be due to the way the polycyclic units (PCUs) are connected to each other in A1 and A2. Although this aspect is discussed below at this point, we mention that Figure 2 shows the rosary-type structure that one could obtain when the PCUs are interconnected through the alkyl chain. These are the types of structures proposed here and elsewhere[11] for molecules comprising fraction A2. These structures are very flexible and can take a large number of folded conformers, two of which are shown in Figure 3. In fact, it is expected that, in toluene and similar solvents, folded conformers should prevail in view of the well-known aggregation tendency of asphaltenes in this solvent. On the other hand, structures such as the one shown in Figure 4, proposed here as a model for fraction A1, cannot fold in the way illustrated for

* To whom correspondence should be addressed. E-mail: soaceved@cantv.net.

(1) Ignasiak, T.; Kemp-Jones, A. V.; Strausz, O. P. The molecular structure of Athabasca asphaltene. Cleavage of the carbon−sulfur bonds by radical ion electron transfer reactions. *J. Org. Chem.* **1977**, *42*, 312−320.

(2) Semple, K. M.; Cyr, N.; Fedorak, P. M.; Westlake, D. W. S. Characterization of asphaltene from cold-lake heavy oil. Variation in chemical structure and composition with molecular size. *Can. J. Chem.* **1990**, *68*, 1092−1099.

(3) Strausz, O. P. Structural features of Atabasca bitumen related to upgrading phenomena. *Prepr.−Am. Chem. Soc., Div. Pet. Chem.* **1989**, *34* (2), 395−400.

(4) Speight, J. G. On the molecular nature of petroleum asphaltenes. In *Chemistry of Asphaltenes*; Bunger, J. W., Li, N. C., Eds.; Advances in Chemistry Series 195. American Chemical Society: Washington, D.C., 1981; Chapter 1, pp 1−15.

(5) Payzant, J. D.; Lown, E. M.; Strausz, O. P. Structural units of Athabasca asphaltenes. The aromatics with a linear carbon framework. *Energy Fuels* **1991**, *5*, 445−453.

(6) Miller, J. T.; Fisher, R. B.; Thiyagarajan, P.; Winans, R. E.; Hunt, J. E. Subfractionation and characterization of mayan asphaltenes. *Energy Fuels* **1998**, *12*, 1290−1298.

(7) Strausz, O. P.; Mojelsky, T. W.; Lown, E. M. Structural features of Boscan and Dury asphaltenes. *Energy Fuels* **1999**, *13*, 228−247.

(8) Murgich, J.; Abanero, J. A.; Strausz, O. P. Molecular recognition in aggregates formed by asphaltene and resins molecules from the Athabasca oil sand. *Energy Fuels* **1999**, *13*, 278−286.

(9) Cimino, R.; Correra, S.; Del Bianco, A.; Lockhard, T. P. In *Asphaltenes. Fundamentals and Applications*; Sheu, E. Y., Mullins, O. C., Eds.; Plenum Press: New York. 1993; Chapter 3, pp 97−126.

(10) Gutiérrez, L. B.; Ranaudo, M. A.; Méndez, B.; Acevedo, S. Fractionation of asphaltene by complex formation with *para*-nitrophenol. A method for structural studies and stability of asphaltene colloids. *Energy Fuels* **2001**, *15*, 624−628.

(11) Acevedo, S.; Escobar, O.; Echevarría, L.; Gutiérrez, L. B.; Méndez, B. Structural analysis of soluble and insoluble fractions of asphaltenes isolated using the PNP method. Relation between asphaltene structure and solubility. *Energy Fuels* **2004**, *18*, 305−311.

10.1021/ef070089v CCC: $37.00
Published on Web 06/01/2007

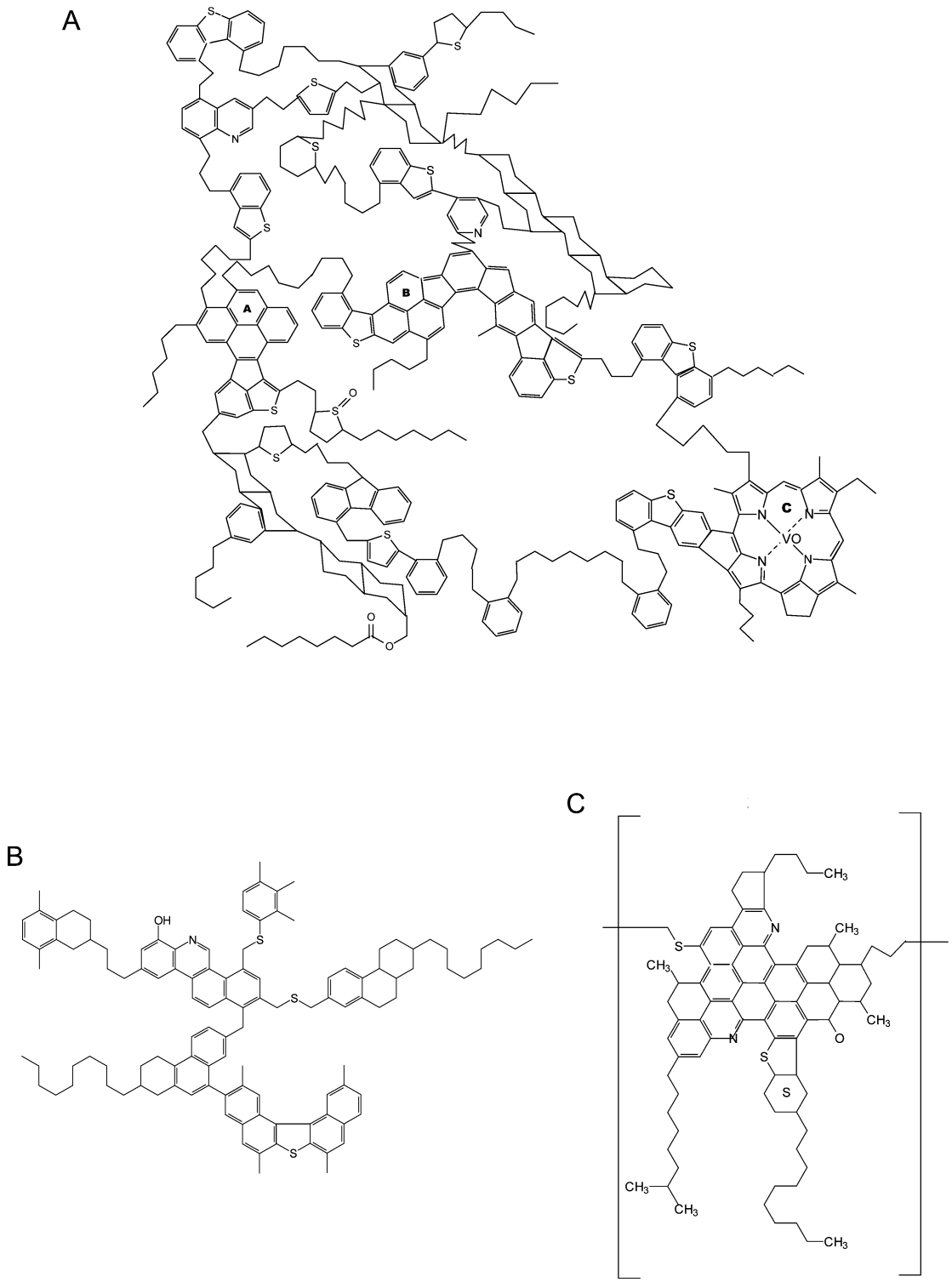

Figure 1. Some hypothetical asphaltene structures proposed on the basis of spectroscopy and measured chemical data: (A) from ref 8, (B) from ref 9, and (C) from ref 4.

A2. As shown in the calculations below, the ability to fold could lead to very large changes in the expected solubility parameter.

Trapping of molecules by asphaltenes in a sort of host−guest complex was proposed to account for the presence of free radicals in petroleum asphaltenes.[12,13] In general, carbon-free radicals are exceedingly reactive species, which are not expected to survive when exposed. Thus, these species should be effectively isolated from the environment by being trapped or caged in asphaltene traps.[12,13] This idea could be extended to any compound that could play the guest role. As suggested earlier,[13] this kind of complex could account for the failure to extract all metallic porphyrines from asphaltenes. Figure 5 is a model that could be suggested for this type of complex. Trapping of saturated hydrocarbons has also been reported by Graciaa et al.[14,15]

(12) Acevedo, S.; Escobar, G.; Ranaudo, M. A.; Piñate, J.; Amorín, A.; Silva, P.; Díaz, M. Observations about the structure and dispersion of petroleum asphaltenes aggregates obtained from dialysis fractionation and characterization. *Energy Fuels* **1997**, *11*, 774−778.

(13) Mujica, V.; Nieto, P.; Puerta, L.; Acevedo, S. Caging of molecules by asphaltenes. A model for free radical preservation in crude oils. *Energy Fuels* **2000**, *14*, 632−639.

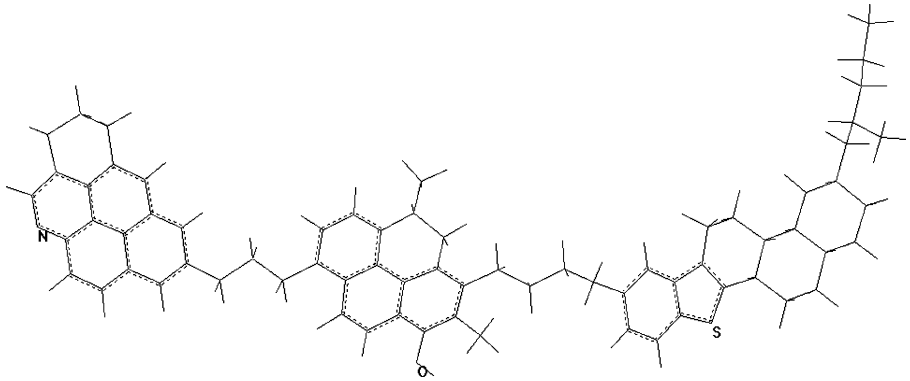

Figure 2. Rosary-type flexible structure for an asphaltene model used to simulate compounds in the soluble fraction A2. A similar structure was proposed earlier.[11]

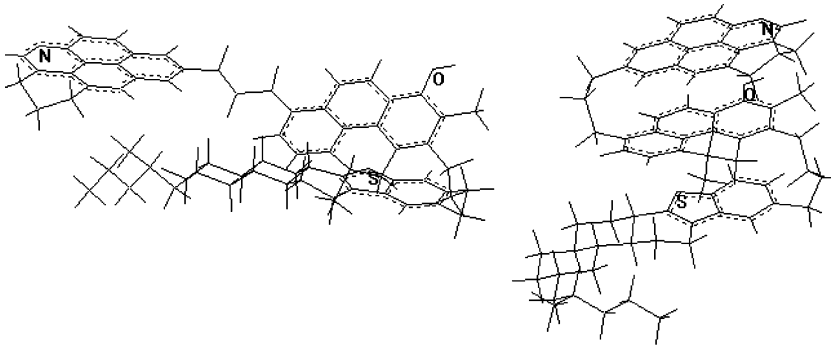

Figure 3. Two-folded conformer of the model shown in Figure 2. Conformers on the left and right are hereafter called conformers I and II, respectively.

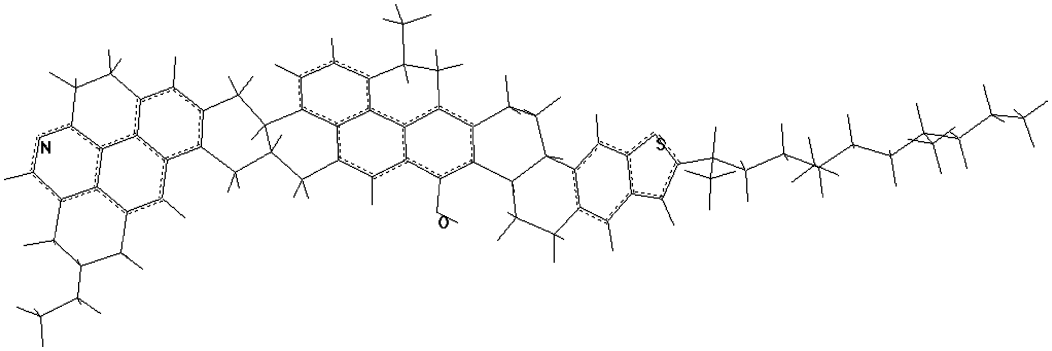

Figure 4. Condensed rigid structure for an asphaltene model expected to be found in fraction A1.

Swelling of asphaltenes by heptane and other solvents was reported by Carbognani and Rogel.[16] According to these authors, such swelling is due to aliphatic chains connecting the above PCUs.

Adsorption studies of asphaltene solutions at both the silica−toluene and glass−toluene interfaces show strong time dependence.[17,18] Besides, it was also observed that the desorption kinetics of Furrial asphaltene from the silica−toluene interface showed a desorption much lower than expected even after 50 h of desorption time.[18] As discussed below, this behavior could be accounted for in terms of equilibrium between folded and unfolded rosary-type structures.

The phase behavior of asphaltenes has been accounted for in terms of chemical-potential equations derived for polymers.[9] Thus, flexible, rosary-type structures are assumed in these treatments. Therefore, on the basis of the Flory theory, Hirschberg et al. used eq 1 below to obtain the asphaltene solubility, as measured by ϕ_2[19]

$$\ln(\phi_2) - \left(\frac{V_2}{V_1} - 1\right) + \frac{V_2}{RT}(\delta_2 - \delta_1)^2 = 0 \qquad (1)$$

Here, ϕ_2 is the volume fraction of asphaltene; V_2 and V_1 are the molar volumes of the solute and solvent, respectively; δ_2 and

(14) Liao, Z.; Graciaa, A.; Geng, A.; Chrostowska, A.; Creux, P. A new low interference characterization for hydrocarbons occluded inside asphaltene structures. *Appl. Geochem.* **2006**, *21* (5), 833−838.

(15) Liao, Z. W.; Geng, A. S; Graciaa, A.; Creux, P.; Chrostowska, A.; Zhang, Y. X. Different adsorption/occlusion properties of asphaltenes associated with their secondary evolution processes in oil reservoirs. *Energy Fuels* **2006**, *20* (3), 1131−1136.

(16) Carbognani, L.; Rogel, E. Solvent swelling of petroleum asphaltenes. *Energy Fuels* **2002**, *16*, 1348−1358.

(17) Acevedo, S.; Castillo, J.; Fernández, A.; Goncalves, S.; Ranaudo, M. A. A study of multilayer adsorption of asphaltenes on glass surfaces by photothermal surface deformation. Relation of this adsorption to aggregate formation in solution. *Energy Fuels* **1998**, *12*, 386−390.

(18) Acevedo, S.; Ranaudo, M. A.; García, C.; Castillo, J.; Fernández, A.; Caetano, M.; Goncalves, S. Importance of asphaltene aggregation in solution in determining the adsorption of this sample on mineral surfaces. *Colloids Surf.* **2000**, *166*, 145−152.

(19) Hirschberg, A.; de Jong, L. N. J.; Schipper, B. A.; Meijer, J. G. Influence of temperature and pressure on asphaltene flocculation. *Soc. Petrol. Eng. J.* **1984**, *24* (3), 283−293.

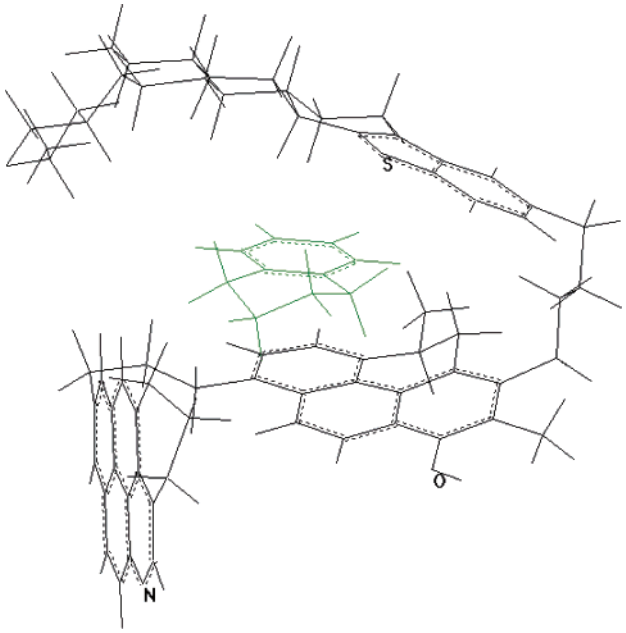

Figure 5. Host−guest model illustrating the trapping of a guest (tetraline) by a folded conformer of the model shown in Figure 2.

δ_1 are the solubility parameters of the solute and solvent, respectively; R is the gas constant; and T is the temperature. This equation is assumed to be valid for $\phi_2 \ll 1$. Manipulation of this equation shows that the solubility ratio ϕ_2/ϕ_3 for two different asphaltene components with the same molar volume could be estimated as

$$\ln(\phi_2/\phi_3) = -\frac{V_2}{RT}[(\delta_2 - \delta_1)^2 - (\delta_3 - \delta_1)^2] \qquad (2)$$

Assuming that both the arbitrary, reference component 3 and solvent have the same solubility parameter, eq 3 is obtained

$$(\phi_2/\phi_3) = \exp\left(-\frac{V_2}{RT}[(\delta_2 - \delta_1)^2]\right) \qquad (3)$$

An equation similar to eq 3 was used here to estimate solubility ratios (see eq 7 below).

It is suggested that the properties above are related to the ability of folding (solubility and trapping) and unfolding (swelling and adsorption) of the flexible rosary-type molecules expected to be present in the soluble fraction A2. In this paper, further evidence, both experimental and theoretical, aiming to sustain the above flexible structures is presented. As shown below in the laser desorption ionization mass spectrometry (LDI MS) and size-exclusion chromatography (SEC) experiments performed, the different adsorption experiments described and the theoretical calculations done are all consistent with the rosary-type structures described. The possible impact of such structures in the conversion of asphaltenes is also mentioned.

Experimental Section

Materials. Asphaltenes from several crude oils were obtained using standard procedures described elsewhere.[20] Resins were thoroughly removed with boiling heptane using a Soxhlet apparatus. When required, resins were obtained from the heptane solution by evaporation of heptane under vacuum. Cerro Negro asphaltene fractions CNA1 and CNA2 (with solubilities equal to 0.09 and 100 g L^{-1}, respectively, in toluene at room temperature) were obtained after treating a solution of Cerro Negro asphaltenes (8 g L^{-1} in toluene) with a toluene-saturated solution of *p*-nitrophenol (PNP) as described earlier.[10] When required, PNP was removed from complexes A1−PNP and A2−PNP after washing their chloroform solutions with aqueous sodium hydroxide. UV−vis spectrophotometry was employed to monitor the aqueous solution for the removal of PNP from asphaltenes.

Mass Spectra. LDI mass spectra were recorded using an Applied Biosystems apparatus (MALDI−TOF Voyager DE-STR) as described earlier.[20] Molecular-weight measurements were performed after optimization of laser shots (LS) for maximum volatilization and minimum fragmentation (see below). Fragmentation of asphaltenes was carried out by increasing LS at a constant laser energy (3 Hz). For this purpose, the LS was changed between 2300 and 3900.

Adsorption. Adsorption isotherms at the silica−toluene interface using both asphaltenes and CNA2 toluene solutions were measured after 72 h, employing a variation of the method described earlier.[18] Solution concentrations in the 0−3000 mg L^{-1} range were used. Commercial thin-layer plates of silica supported on Teflon was used as the adsorption surface. The amount adsorbed was determined by the change in the solution absorbance using a Stellar Net EPP 2000 apparatus. Calibration curves were determined using four different optical paths: 1 cm for solutions between 5 and 400 mg L^{-1}, 0.5 cm for solutions between 200 and 600 mg L^{-1}, 0.2 cm for solutions between 400 and 1500 mg L^{-1}, and 0.1 cm for solutions between 1000 and 3000 mg L^{-1}. Calibration straight lines were obtained in all cases, with correlation coefficients ≥ 0.99. The amount of sample adsorbed ν_A, measured in milligrams of sample per gram of silica, was calculated from eq 4

$$\nu_A = \frac{CV_S}{1000w} \qquad (4)$$

In this equation, C is the solution concentration in mg L^{-1}. It was obtained from the final absorbance using the calibration curve. V_S in milliliters is the volume of solution actually measured, and w is the weight of silica (≥ 0.09 g in all cases).

Desorption experiments were carried out as follows: after the adsorption time (72 h), the plate was removed from the solution, dipped in fresh toluene to removed any solution film, and then placed in clean toluene. Barely any asphaltene was detected in the dipping solution. The amount of desorbed sample after 72 h was then measured as usual.

The parameter S_A or the apparent solubility of asphaltene in toluene when the sample is in contact with silica was estimated as follows: let ν_A be the amount of asphaltene adsorbed in the plate after 72 h, taken here to be equal to the initial surface concentration in the plate for the desorption experiment.

Let ν_D be the final surface concentration in the desorption experiment. Let C_E be the expected solution concentration obtained from the adsorption isotherm. In other words, in the adsorption isotherm curve, C_E is the solution concentration corresponding to ν_D. Let C_D be the measured solution concentration corresponding to ν_D in the desorption experiment. Then, the parameter S_A or the apparent solubility of the sample in contact with the silica surface was calculated from eq 5

$$S_A = \frac{C_D}{C_E}S_0 \qquad (5)$$

In this equation, S_0 is the solubility of the asphaltene sample in toluene at room temperature (saturated solution near 100 g L^{-1}). The meaning of ν_A, ν_D, C_E, and C_D is illustrated in Figure 6.

SEC. SEC experiments were carried out in a Waters high-performance liquid chromatography (HPLC) model 484, provided with a UV detector working at 250 nm. Two Ultrastyragel columns, described by the manufacturer as 500 and 100 Å with dimensions of 7 mm wide and 300 mm long, were used. Tetrahydrofuran (THF)

(20) Acevedo, S.; Gutiérrez, L. G.; Negrin, G.; Pereira, J. C.; Méndez, B.; Delolme, F.; Dessalces, G.; Broseta, D. Molecular weight of petroleum asphaltenes: A comparison between mass spectrometry and vapor pressure osmometry. *Energy Fuels* **2005**, *19*, 1548−1560.

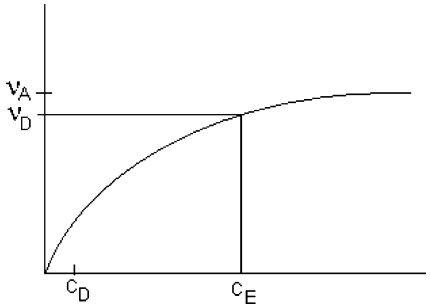

Figure 6. Scheme of an adsorption isotherm employed to illustrate the meaning of ν_A, ν_D, C_E, and C_D. ν_A is the amount of sample adsorbed on the silica after a time t. When the plate is again placed in fresh toluene and allowed to desorb during the same time t, the amount ν_D remains adsorbed. According to the adsorption isotherm, the expected amount in solution should be C_E. However, the much smaller C_D was measured (see the text).

Table 1. Properties of Crude Oil and Asphaltene Samples Examined

crude	API (deg) oil	percentage of asphaltenes in oil	elemental analysis of asphaltene C	H	N	S	H/C	DBE[a]
DM 153[b]	14	10	81.05	8.17	1.64	6.6	1.2	40
CN[b]	8	13	81.22	7.72	2.13	5.5	1.12	43
CNA1			80.78	7.66	1.92		1.14	43
CNA2			80.75	8.38	1.8		1.25	38
Ceuta	29−32	2	86.46	6.96	1.34	3.01	0.97	52

[a] Double bonds equivalent per 100 carbon atoms estimated from eq 8. [b] From ref 20.

was employed as the mobile phase. The system was calibrated with polystyrene standards, and a linear range between about 20 000 and 500 nominal mass was established. Very diluted asphaltene solutions (less than 100 mg L^{-1}) were used in these experiments.

Molecular Mechanics and PM3 Calculations. These were performed using the MM+ and PM3 program from Hyperchem software. MM+ is a molecular mechanics program, and PM3 is a semiempirical quantum mechanics program. Energy optimizations were calculated using a Polak−Ribiere algorithm and a gradient equal to 0.1. The QSAR program was employed to obtain van der Waals molecular volumes. A procedure, similar to the one reported,[11] was used to calculate solubility parameters Δ using eq 6

$$\Delta = \left(\frac{-\Delta E_D}{V}\right)^{1/2} \tag{6}$$

In this equation, ΔE_D is the formation energy of the dimer and V is the molecular volume.

PM3 was used to estimate ΔE_f, the heats of formation of radicals.

On the basis of the Hirschberg treatment described above (see eq 3), solubility ratios between two models 1 and 2 were estimated using eq 7

$$\Delta S_R = \exp\left(-\frac{V}{RT}(\Delta_2 - \Delta_1)^2\right) \tag{7}$$

Results

Material Properties. Table 1 shows some properties of crude oils and asphaltenes used in this work. On American Petroleum Institute (API) gravity grounds, the oils are classified as extra-heavy (CN), heavy (DM-153), and medium (Ceuta). As shown in this table, elemental analyses are for asphaltene samples. Double-bond equivalents per 100 carbon atoms were estimated using eq 8, where C is the number of carbons (100) and H and N are the number of hydrogens and nitrogens, respectively

$$\mathrm{DBE} = \frac{2C + 2 - H - N}{2} \tag{8}$$

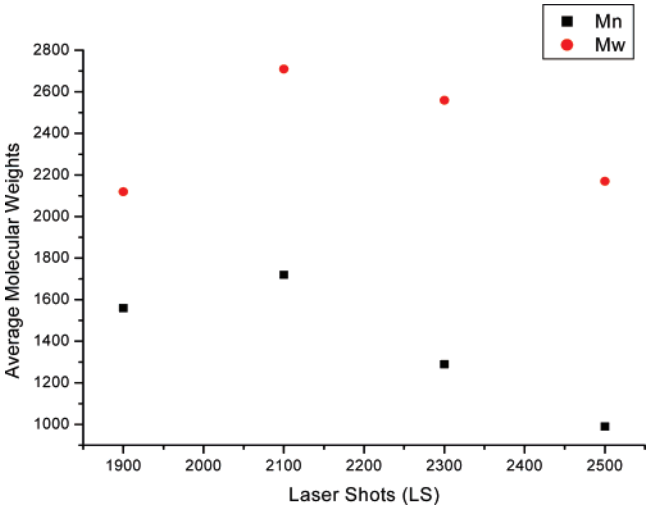

Figure 7. Change of M_n (lower values) and M_w for DM-153 with LS. This experiment is performed to find the optimum LS required to measure the average molecular weights. Too low and too high of LS lead to too low of averages because of either incomplete volatilization (too low of LS) or excessive fragmentation (too high of LS).

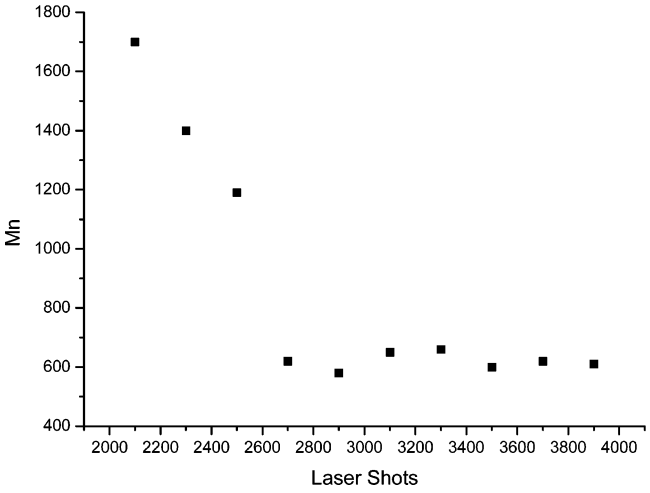

Figure 8. Change of M_n with the number of laser shots for Cerro Negro asphaltenes.

Note the DBE difference between CNA1 and CNA2 samples.

Mass Spectra. As discussed earlier, the measuring of molecular mass requires optimization of the laser energy or laser shot (LS).[20] Using a too low LS value leads to incomplete volatilization, which in turn leads to too low molecular-mass averages; on the other hand, fragmentation of a too high LS value also leads to too low values. These effects are shown in Figure 7 for a DM 153 asphaltene, where maxima are clearly observed. Similar curves were obtained for other asphaltenes samples (CN and Ceuta).

As suggested by the results in Figure 7, the best choice for LS is the value corresponding to the maximum average molecular weight obtained, equal to 2100 for this and other asphaltenes samples examined. An identical LS value was selected previously for the measurements of M_n and M_w for several asphaltenes based on this and other criteria.[20]

To examine how the M_n value drops from its maximum as LS is increased, Figure 8 was constructed for the CN sample. As shown in this figure, the M_n value drops with LS until a sort of limiting M_n is reached (close to 600). A further increase of LS beyond the value corresponding to this limit does not lead to any significant decrease of M_n. Similar results were obtained for DM 153 and Ceuta asphaltenes.

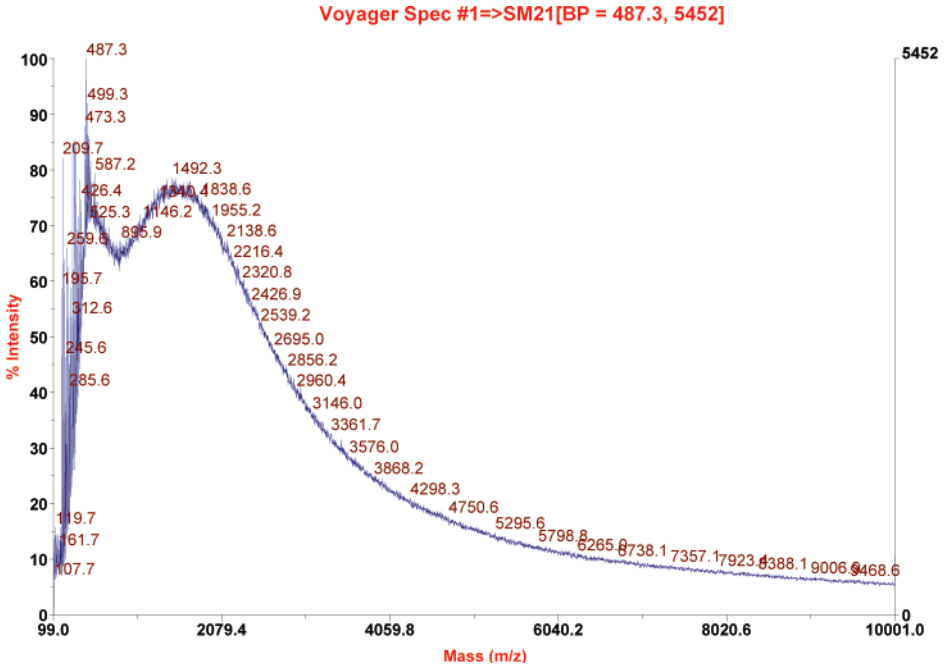

Figure 9. LDI spectra of VLA 711 asphaltene measured in the *m*/*z* 100−10 000 range using LS = 2100. It is important to note the bimodal nature of the MWD. Reprinted from ref 20.

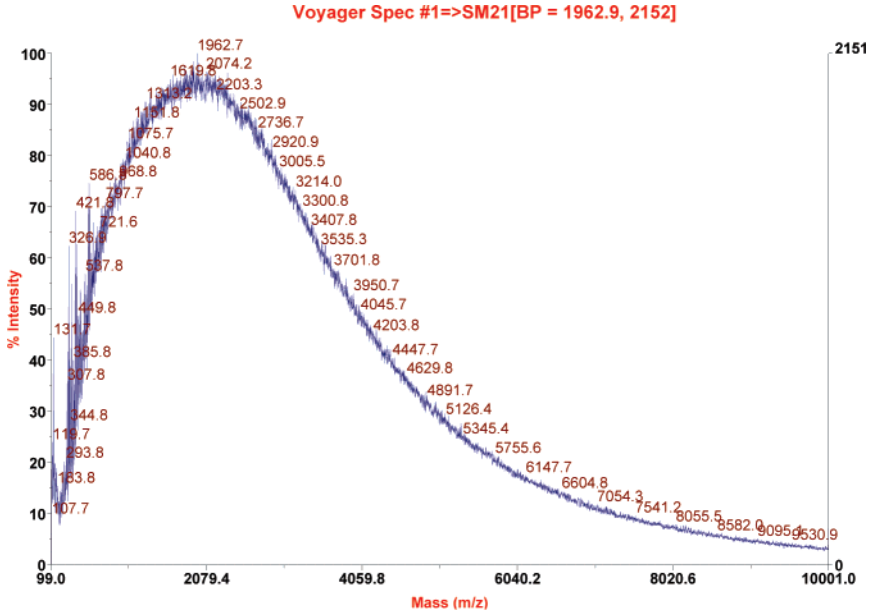

Figure 10. LDI spectra of VLA 711 octylated asphaltene measured in the *m*/*z* 100−10 000 range using LS = 2100. It is important to note the unimodal nature of the MWD. Reprinted from ref 20.

Figures 9 and 10 correspond to the reported[20] LDI MS of the VLA 711 asphaltene sample and octylated asphaltene derivative. They are reproduced here for convenience. As shown in Figure 9, the molecular-weight distribution (MWD) of this sample is clearly bimodal. Similar bimodal MWDs were reported for other asphaltenes.[20] A comparison of Figures 9 and 10 suggest that these bimodal distributions are not due to sample fragmentation.

Figure 11 corresponds to the LDI MS taken for resins from Cerro Negro (CNR). The spectrum was recorded using the same conditions employed for asphaltenes. The numerical results are shown in Table 2, and contrary to what was observed for asphaltenes, the average values do not show the dependence with LS shown in Figure 8. The average of M_n and M_w values obtained for each LS value leads to a very small standard deviation (see Table 1). The CNR spectra (Figure 11) changed little when LS was increased. In particular, the intensity of a series of bands in the interval between approximately *m*/*z* 300 and 600 increased with LS. As suggested earlier, this is likely to be due to the polymerization of some resin components.[21]

(21) Tanaka, R.; Sato, S.; Takanohashi, T.; Hunt, J. E.; Winans, R. E. Analysis of the molecular weight distribution of petroleum asphaltenes using laser-desorption mass spectrometry. *Energy Fuels* **2004**, *18*, 1405−1413.
(22) Bergmann, J. G.; Duffy, L. J. Solvent effects in GPC. *Anal. Chem.* **1971**, *43*, 131−133.
(23) Haley, G. A. Molecular and unit sheet weights of asphalt fractions separated by GPC. *Anal. Chem.* **1971**, *43*, 371−375.
(24) Reerink, H.; Lijzenga, J. GPC calibration curve for asphaltenes and bituminous resins. *Anal. Chem.* **1975**, *47*, 2160−2167.

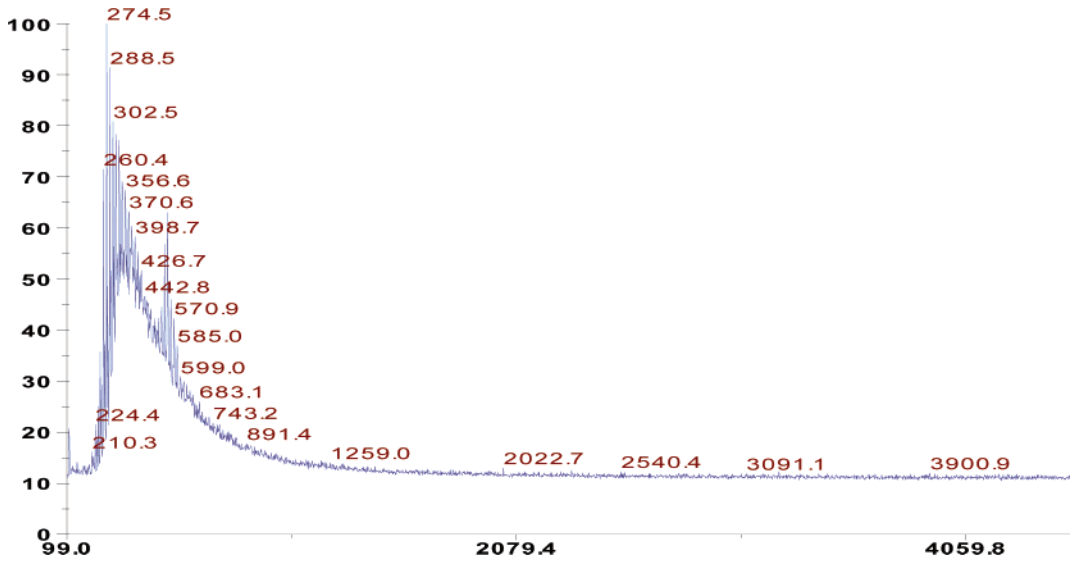

Figure 11. LDI spectra of a resin sample isolated from Cerro Negro crude oil (see the Experimental Section). Conditions are the same as in Figure 9.

Table 2. M_n and M_w Values Measured for Cerro Negro Resins Using Different LS Values

LS	M_n	M_w
2100	760	1270
2300	770	1130
2500	730	1240
average	753 ± 21	1213 ± 74

However, for the LS range examined, no significant impact of this effect was noted on the spectra recorded and on the values measured (Table 2).

SEC. Figure 12 shows the SEC of the three samples analyzed: CN (coded asphaltenes) and the corresponding A1−PNP (coded A1) and A2−PNP (coded A2) complexes. In all chromatograms shown, the first wide band with a retention time around 11.4 min corresponds to asphaltenes (see the chromatogram on the top of Figure 12); two bands near 18.5 and 21 min correspond to contaminants present in the sample. The band close to 17.5 min, in both chromatograms coded as A1 and A2, corresponds to *free* PNP, and the band at 15.43 min in A2 corresponds to associate PNP. Determination of the free PNP band was achieved after injection of complex samples with different amounts of PNP. It is important to note that the band near 15.4 min in the A2 chromatogram is *not present* in chromatogram A1. The terms free and associated PNP are relative, qualitative terms employed here to distinguish between PNP in solution and PNP trapped within asphaltene sheets.

The different retention times between associated and free PNP could be accounted for as follows: when the diluted solution of complex A2−PNP is injected in the column, both the PNP in solution (free) and the one trapped in asphaltenes (associated) are in equilibrium. By the effect of the mobile-phase flux and in view of its much higher volume, the complex will move faster than the free PNP in the column. As a result of the above physical separation between the complex and free PNP, the equilibrium between the two is broken and the complex will try to re-establish the equilibrium by dissociating and liberating the trapped PNP. Finally, two bands of PNP reach the detector at two different retention times. These processes are schematized in Figure 13.

Adsorption Experiments. Figure 14 shows the adsorption isotherms corresponding to the two samples studied: Cerro Negro asphaltenes (CN) and the corresponding soluble fraction of this asphaltene (CNA2). The points are averages of at least two measurements, and as suggested by the error bars, reproducibility was good enough. Similar results have been reported earlier for other asphaltenes in the same system (toluene−silica).[27,28]

Table 3 shows the results of the adsorption and solubility analysis performed with sample CNA2. As explained above, S_A values are estimates of the solubility of the CNA2 sample when adsorbed on the silica surface. As shown in this table, these values are weakly dependent upon the concentration and lead to the average for S_A equal to 1.3 ± 0.3 g L^{-1}. Accordingly, solubility is reduced near 77-fold. Similar results were found for CN where a solubility reduction near 58-fold was observed.

Molecular Mechanics (MM) Calculations. MM calculations were performed using the models shown in Figures 2 and 4 above. Although, generally speaking, these models have some features commonly found in asphaltenes, these were chosen by convenience. Model A2 is similar to the one discussed earlier.[11] They have a similar molecular weight, H/C ratio, and fraction of aromatic carbons (see Table 4).

The procedure employed to obtain the parameter Δ defined in eq 6 was the same used before except that molecular volumes were calculated using the QSAR program of the commercially available HyperChem package. As shown earlier,[11] a fair linear correlation between the experimental solubility parameter δ and Δ could be obtained when the energy corresponding to the dimer or other aggregates of the models is used in eq 6 to obtain Δ. Table 5 shows the calculated parameter for the studied models

(25) Sato, S.; Takanohashi, T. Molecular weight calibration of asphaltenes using gel permeation chromatography/mass spectrometry. *Energy Fuels* **2005**, *19*, 1991−1994.

(26) Acevedo, S.; Escobar, G.; Ranaudo, M. A.; Rizzo, A. Molecular weight properties of asphaltenes calculated from GPC data for octylated asphaltenes. *Fuel* **1998**, *77*, 853−858.

(27) Acevedo, S.; Ranaudo, M. A.; García, C.; Castillo, J.; Fernández, A.; Caetano, M.; Goncalves, S. Importance of asphaltene aggregation in solution in determining the adsorption of this sample on mineral surface. *Colloids Surf.* **2000**, *166*, 145−152.

(28) Castillo, J.; Fernández, A.; Ranaudo, M. A.; Acevedo, S. New techniques and methods for the study of aggregation, adsorption and solubility properties of aspahltenes. Impact of these properties on colloidal structure and flocculation. *Pet. Sci. Technol.* **2001**, *19* (1 and 2), 79−110.

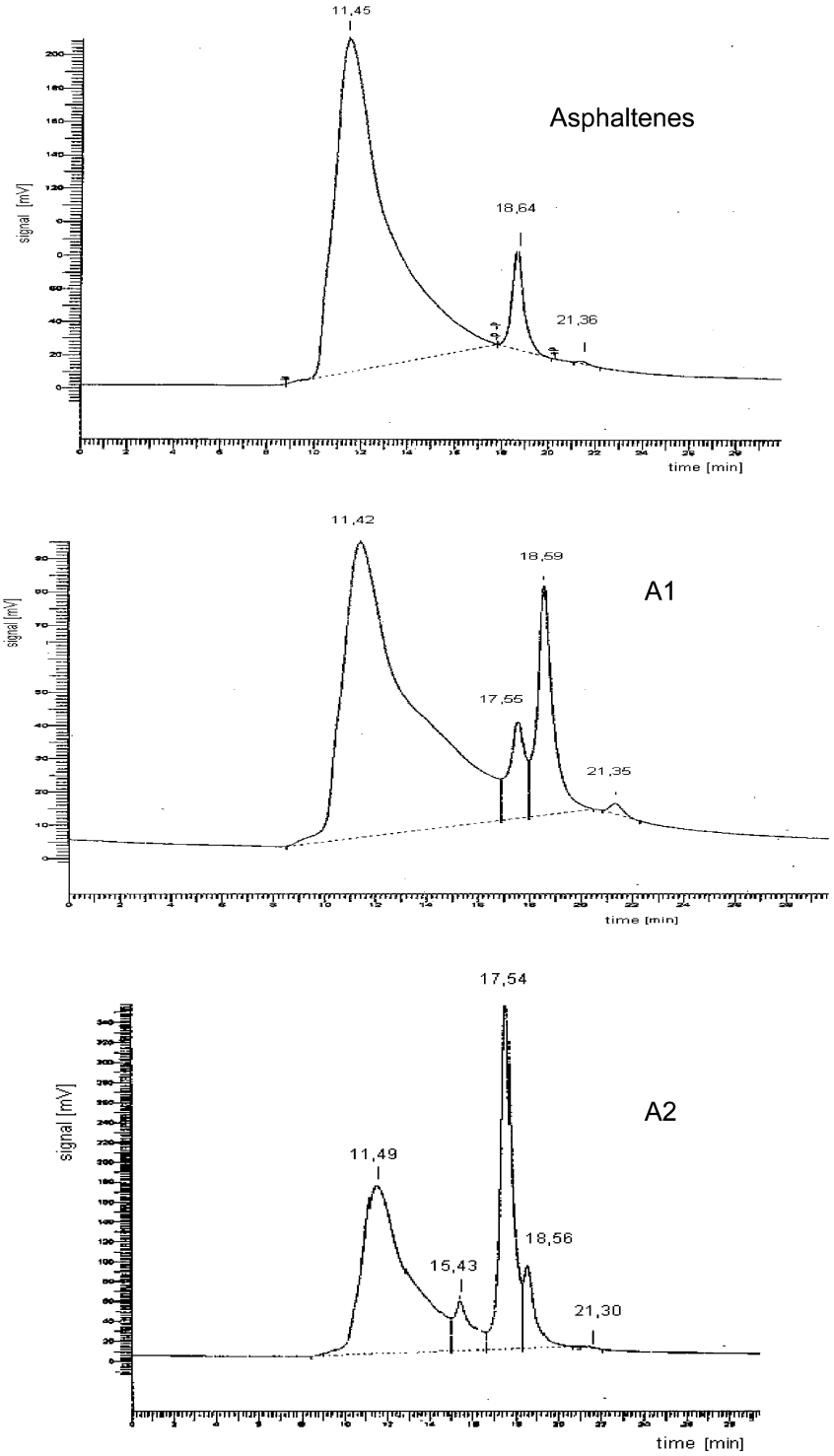

Figure 12. SEC of asphaltenes and A1 and A2 fractions.

A1 and A2. Also, an estimation of the solubility ratio ΔS_R obtained using eq 7 and $\Delta_1 = 9.25$ MPa$^{0.5}$ (toluene) is included in the table.

Discussion

The results described above could all be accounted for in terms of the rosary-type structures described. The fragmentation shown in the mass spectra shown in Figure 8 is certainly consistent with this type of structure. Apparently, aliphatic chains connected to aromatic units are weak enough to be broken by the absorbed energy from the laser. The idea is illustrated in Table 6 and Figure 15 with three model compounds. Calculations correspond to the following homolitic rupture of the corresponding C−C bond:

$$R-CH_2-CH_2-R' \rightarrow R-CH_2\bullet + \bullet CH_2 - R'$$

As shown in Table 6, the rupture is favored when R and R′ are both aromatic rings.

As can be shown by calculations with other models, the above differences $\Delta\Delta E_f$ are expected to increase with larger ring systems containing heteroatoms.

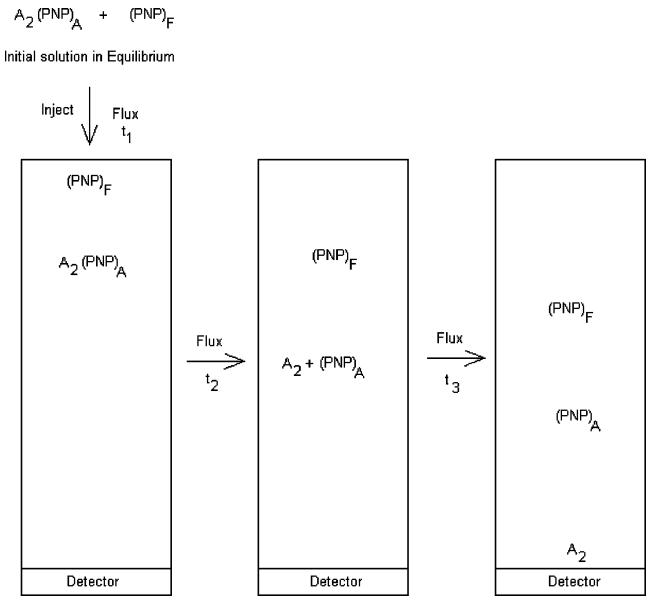

Figure 13. Scheme representing events in the SEC experiment with the complex A2−PNP. On the left at the top, the complex is in equilibrium with free PNP in solution $(PNP)_F$; after injection (time t_1), the flux moves the complex down the column and away from PNP in solution. In the center, after a time t_2, the complex is dissociated, affording A2 and associated PNP, $(PNP)_A$. On the right, after a time t_3, A2 reaches the detector; this will be followed by $(PNP)_A$ and then by $(PNP)_F$. See the text for more details.

The plateau obtained in Figure 8 after LS = 2600 suggests that at this point all relatively weak bonds are broken. As shown in Figure 8, a significant drop in M_n from about 1700 to 600 is produced by fragmentation.

It is interesting that resins analyzed do not show the fragmentation observed for asphaltenes when LS is increased (see Table 1 and Figure 11). A similar behavior was reported earlier by Tanaka et al.[21] According to the discussion above, this would be the expected result for compounds with lower aromatic and lower heteroatom content than asphaltenes, as is the case for resins.

Table 3. Desorption[a] and Solubility Corresponding to Sample CNA2

υ_D[b] (mg g^{-1})	C_D[c] (mg L^{-1})	C_E[d] (mg L^{-1})	S_A[e] (g L^{-1})
63.85	6	604	0.99
73.68	11	752	1.46
89.03	15	1100	1.36
120.05	18	1595	1.13
177.28	24	1964	1.22
205.97	36	2289	1.57

[a] Desorption at the silica−toluene interface at room temperature, measured after 72 h. [b] Amount of asphaltene adsorbed remaining in the plate after the desorption experiment. [c] Amount in solution actually measured in the desorption experiment. [d] Expected amount in solution. [e] Solubility of the sample adsorbed, estimated using eq 5 and S_0 = 100 g L^{-1}. See the Experimental Section and Figure 6 for more details regarding these parameters.

Table 4. Common Features of Models A1 and A2 Used in This Work

M_w (g mol^{-1})	C	H	N	O	S	H/C	f_a[a]
966.4	69	75	1	1	1	1.09	0.53

[a] Fraction of aromatic carbons.

Table 5. Calculated Parameters for Models A1 and A2

model[a]	$-\Delta E_D$ (J mol^{-1})[b]	V (cc)	Δ (MPa$^{0.5}$)[c]	ΔS_R[d]
A1	203 649	933	14.77	0.000 01
A2 unfolded	204 569	949	14.68	0.000 01
A2 conformer I	141 284	949	12.2	0.036
A2 conformer II	81 092	947	9.25	

[a] Structures of these models are shown in Figures 4 (A1), 2 (A2), and 3 (conformers I and II). [b] Energy of dimer formation. [c] Calculated from eq 6. [d] Calculated from eq 7 using Δ_1 = 9.25 MPa$^{0.5}$.

The aging effects illustrated by the adsorption and desorption experiments could easily be accounted for in terms of the folding−unfolding properties of the rosary-type structures. It is reasonable to suggest that after adsorption the silica surface promotes unfolding of conformers at the interface. That is, after diffusion-controlled adsorption of folded conformers, a slow unfolding process at the surface is promoted by the surface, leading to a much lower that expected desorption. As measured

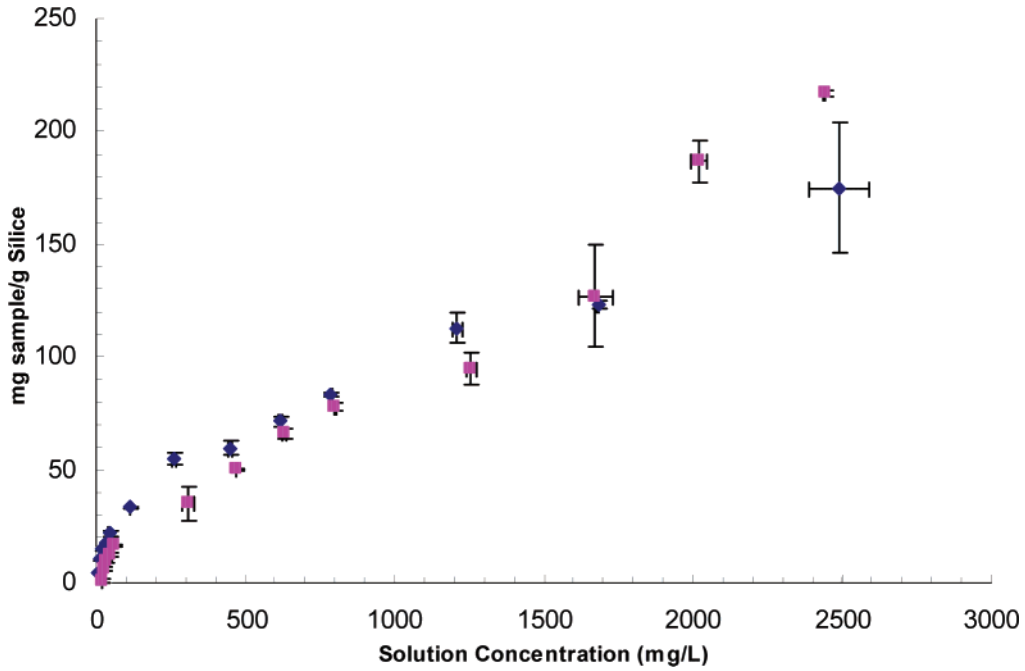

Figure 14. Adsorption isotherms corresponding to CNA (squares) and CNA2 (rhombi). Adsorption at the silica−toluene interface at room temperature. Measured after 72 h.

Table 6. Heats of Formation of Radicals ΔE_f and Differences $\Delta\Delta E_f$ for Three Model Compounds, Calculated Using PM3

model	ΔE_f[a]	$\Delta\Delta E_f$[a,b]
1,2-diphenyl etane	39.5	0
1-phenyl-2-ciclohexil etane	49.25	9.8
dicyclohexyl etane	58.27	18.8

[a] Units in kcal mol^{-1}. [b] Differences with respect to 1,2-diphenyl etane.

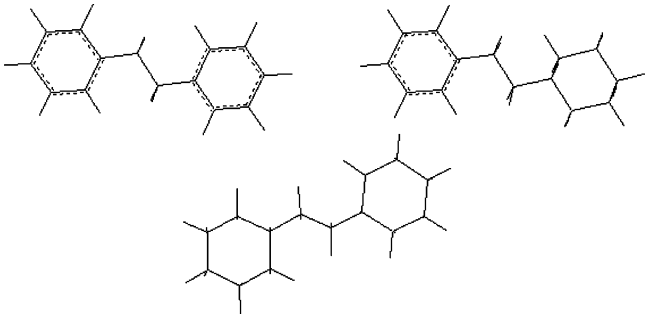

Figure 15. From top and clockwise, 1,2-diphenyl etane, 1-phenyl-2-ciclohexyl etane, and 1,2-diclohexyl etane.

by the parameter S_A (eq 6), the effect could be very large. Thus, after 72 h, this reduction is close to 100-fold. As mentioned in the Introduction, the strong time dependence of asphaltene adsorption has been reported earlier.

As suggested by the large ν_A values shown in Figure 14, there appears to be little doubt that the asphaltene surface is a multilayer. Building of such a multilayer is possible because the surface is continuously depleting the folded conformer adsorbed. Thus, as time goes by, droved by the tendency of the system to achieve an equilibrium, more folded conformer is adsorbed. Such a mechanism is an attractive one to account for the formation of macroscopic layers of asphaltenes deposited on facility productions.

The SEC experiments performed in this work showed very clearly that fraction A2 is more effective than A1 in trapping PNP molecules. The hypothetical flexible nature of A2, simulated by means of the model above (Figure 2), allows for the type of host−guest complex modeled in Figure 5. The band at 15.43 min, present in the SEC, corresponding to the A2−PNP sample and conspicuously absent in the A1−PNP sample, strongly suggests that PNP is trapped very effectively by A2. The trapping is so effective that after many PNP extractions (see the Experimental Section) the above band remained in SEC after the band at 17.54 min has long disappeared.

The bimodal nature of the MWD shown in Figure 9 is consistent with the molecular trapping discussed above. Apparently, the band located in the lower MW range is due to compounds trapped by asphaltenes. Because asphaltenes were thoroughly washed to remove resins, this band is not due to loosely bound compounds that usually coprecipitate with asphaltenes during the separation from crude oil (see the Experimental Section). These arguments are supported by the SEC shown in Figure 12, where the observed tailing of the wide band could again be accounted for in terms of relatively low MW compounds trapped in the samples. Similar tailing using similar conditions are well-known in the literature.[22−26] Such tailing is reduced extensively when asphaltenes are octylated, affording SEC with almost perfect Gaussian bands.[26] Apparently, during the octylation process, trapped compounds are removed from the sample. This is consistent with the MWD of the octylated sample shown in Figure 10.

Molecular Mechanics. Because van der Waals energies depend a lot on the number of atoms, $-\Delta E_D$ values for models A1 and A2 with the same atoms and number of atoms are very similar (see Table 5). Thus, high $-\Delta E_D$ values should be expected for both rigid molecules and unfolded conformers. Thus, unfolded conformers are expected to have a relatively low solubility (high Δ, see Table 5). On the contrary, folded conformers are expected to have high solubilities and the difference with the unfolded ones could be very large. This is suggested by the very small ΔS_R calculated using eq 7 (see above and Table 5). Although the calculation in Table 5 was done under vacuum, the solubility ratio between A1 and A2 fractions in toluene is indeed very small (around 0.0009). The above results reinforce the trapping hypothesis suggested earlier.

A look to the DBE difference between low-soluble (CNA1) and soluble (CNA2) in toluene samples in Table 1 is instructive. According to the above arguments, it is very likely that this difference is partially or totally due to differences in the way the PCUs are connected. For the soluble sample, they are connected by flexible chains, whereas for the low-soluble sample, they are connected by rings.

Conclusions

The consistence of the rosary-type structure with the different experimental and theoretical results and data from the literature described here is very good news. We believe that in the extremely complex field of the asphaltene structure it is very important to have general rules that, details apart, could give ideas as to the expected behavior of asphaltenes. As described above, important asphaltene phenomena, such as solubility, adsorption, trapping of molecules, swelling, colloidal structure and stability, and MWD in both LDI and SEC, could all be accounted for in terms of these flexible structures.

Finally, the fragmentation experiments above suggest that, when properly treated, asphaltenes could be broken down to valuable products of lower MW.

Acknowledgment. We thank Mr. Edgar del Carpio G. for the adsorption measurements and Lic. Betilde Segovia for administrative assistence. We also thank the Venezuelan−French PCP research program (Asphaltene Proyect), FONACIT (G2005000430), and CDCH (AI-03-12-5509-2004, PG-03-00-5732-2004, and PI-03-00-5648-2004 projects) for financial support.

Nomenclature

A1 = Low-solubility fraction of asphaltene. Solubility is less than $\approx$100 mg L^{-1} in toluene at room temperature.
A2 = Asphaltene fraction soluble in toluene. Solubility is higher than $\approx$5−100 g L^{-1} in toluene at room temperature.
A1−PNP = Insoluble complex formed when a toluene solution of asphaltene (8 g L^{-1}) is mixed with a saturated solution of PNP in toluene.
A2−PNP = Soluble complex formed when a toluene solution of asphaltene (8 g L^{-1}) is mixed with a saturated solution of PNP in toluene.
C = Solution concentration (g L^{-1})
C_D = Measured solution concentration corresponding to ν_D in the desorption experiment (g L^{-1})
C_E = Expected solution concentration corresponding to ν_D (g L^{-1})
CN = Cerro Negro asphaltenes
CNA1 = A1 fraction of Cerro Negro asphaltenes
CNA2 = A2 fraction of Cerro Negro asphaltenes
CNR = Cerro Negro resins, isolated during the purification of CN asphaltenes
DBE = Double-bond equivalent
ΔE_D = Energy formation of the dimer calculated from two monomers (J mol^{-1})

ΔE_f = Heat of formation of radicals, calculated using the PM3 software
LDI = Laser desorption ionization
LS = Laser shots or laser pulses impinging on the sample in a unit time
M_n = Number-average molecular weight
M_w = Weight-average molecular weight
MW = Molecular weight
MALDI−TOF = Matrix-assisted LDI with a time-of-flight detector
MM+ = Molecular mechanics software
PCUs = Polycyclic units in an asphaltene molecule. The cyclic could be aromatic, naphtenic, or both.
PM3 = Semiempirical quantum mechanics software
PNP = *p*-Nitrophenol
R = Gas constant (8.3057 J mol^{-1} K^{-1})
QSAR = Program used to obtain molecular volumes
S_A = Apparent solubility in toluene at room temperature when the asphaltene sample is in contact with a silica surface (g L^{-1})
S_0 = Solubility of asphaltene in toluene at room temperature (g L^{-1})
S_R = Solubility ratio
SEC = Size-exclusion chromatography
T = Temperature (K)
THF = Tetrahydrofurane
V = Molar volume (cm^3)
V_S = Solution volume (cm^3)
w = Weight of silica (g)

Greek Symbols

δ = Solubility parameter ($MPa^{1/2}$)
Δ = Solubility parameter calculated in this work ($MPa^{1/2}$)
ϕ = Volume fraction
ν_A = Amount of asphaltene adsorbed at the silica−toluene interface at room temperature after 72 h (mg g^{-1})
ν_D = Final surface concentration of asphaltenes in the desorption experiment (mg g^{-1})

EF070089V